Copyright © 2005 by ABCM

DESIGN OF A THREE AXIAL TRANSDUCER OF FORCE AND MOMENT FOR AMPUTEE GAIT ANALYSIS

Luciano Santos Constantin Raptopoulos
Program of Mechanical Engineering – PEM/COPPE/UFRJ
e-mail: luciano@mecanica.coppe.ufrj.br

Max Suell Dutra
Program of Mechanical Engineering – PEM/COPPE/UFRJ
e-mail: max@mecanica.coppe.ufrj.br

Fabricio Lopes e Silva
Program of Mechanical Engineering – PEM/COPPE/UFRJ
e-mail: fabrous@click21.com.br

Abstract: *The consequence of the amputation is not only physical but also functional. The gait analysis in amputee subjects is an important way to adjust and align the prosthetics device. The measurement of kinematics and kinetics variables can help in this work. This paper describes the development of a three-axial force and moment transducer for amputee gait analysis. In order to device the three-axial transducer, the procedures are performed as follows: first, the equations between loads and strains are determined; second, the strain gauges arranged and six full Wheatstone bridges are defined; third, the calibration of the transducer is made; and last, a test in an above-knee amputee is performed. Results from the tests that were administrated to the amputee are presented. The calibration and test results provided the applicability of this kind of transducer for amputee gait analysis.*

Keywords*: Three-axial transducer of forces and moments, Amputee gait analysis, Prosthetic loading, Measurement systems.*

1. Introduction

The analysis of the dynamical forces and moments acting on the lower limb amputee using prosthetics devices can help the orthopedic technician in the correct adjustment and alignment of the prosthesis, providing maximal restoration of functionality during the gait cycle.

Three-axial transducers of force and moments have been designed for robots and machines devices, structural investigation and biomechanics analysis, among others. Cunningham and Brown (1952) designed and applied four three-axial pylon transducers as sensor elements of a force plate. These transducers were built with strain gauges and this platform was used in gait analysis. In 1969, at the Bioengineering Unit, University of Strathclyde, Lower designed a pylon transducer in order to analyze knee mechanics (Lower, 1969). Berme *et al.* (1976) built a short pylon transducer to measure prosthetic forces and moments during amputee gait. This transducer was build with six full Wheatstone bridges fixed on the surface of an aluminium bar. Kim *et al.* (1884) designed a three-component load cell by using parallel plate structure. Ono and Hatamura (1986) developed a new three-axial load cell for measuring forces and moments, which was build through two parallel plates. Hatamura and Matsumoto (1989) designed another configuration of multi-component load cell with one radial plate to measure moments, and one parallel plate to measure forces. In 1990, Yabuki developed a six-component force sensor using parallel plates for controlling the robots. Schwarzinger *et al.* (1992) designed and built a gripper that can measure the components of force and moments and was used to help the control system of one manipulator. Chao *et al.* (1999) presented a six-component force sensor to measure the loading of the feet in locomotion. Kim *et al.* (1999) designed and fabricated a multi-component force sensor with the plate-beams, which may be used in industry for measuring forces and moments simultaneously. Kim *et al.* (2003) presented a project of a strain gauge column type multi-component force and moment sensor.

This paper describes the design, calibration and tests of a three-axial force and moment transducer to be used in amputee gait analysis.

2. Methods

2.1. Three-axial transducer design

The three-axial transducer of force (F_x, F_y, F_z) and moments (M_x, M_y, M_z) was built through a short part of aluminium tube with internal diameter d and external diameter D. It is the same tube used in the prosthetic devices.

Twenty-eight strain gauges were used as sensing elements and were fixed on three levels (*Z1*, *Z2*, *Z3*) and along longitudinal lines orientated to each 45º (Fig. 1). The relative space between these levels is 10 mm.

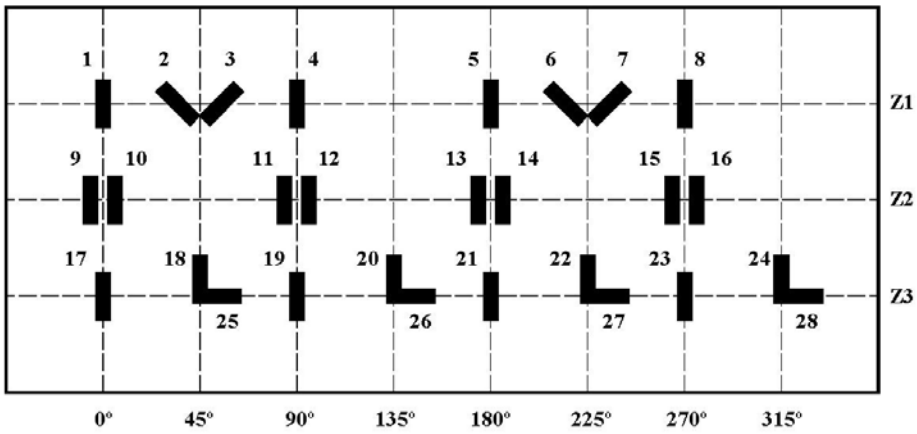

Figure 1. Strain gauges location (cylindrical surface)

The gauges were arranged in six full Wheatstone bridges (Figure 2) with output voltage V_{on} (n = 1…6) and supply voltage V_s.

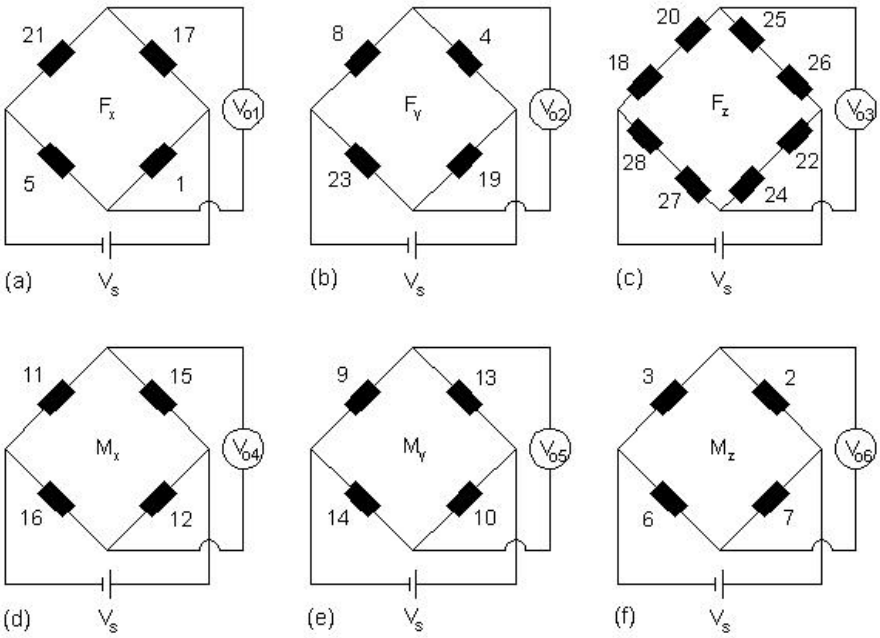

Figure 2. Wheatstone bridges configurations.

2.1.1. Theoretical output of the F_x Wheatstone bridge

The measurement of the force F_x is performed by a full Wheatstone bridge, which is composed by the strain gauges number 1, 5, 17 and 21. These gauges were fixed on levels *Z1* and *Z3* in order to eliminate the influence of the moment M_y in the output of the circuit V_{o1}. The strain ε_1, ε_5, ε_{17} *and* ε_{21} of the gauges 1, 5, 17 and 21, respectively, can be calculated by (1) and (2), where E is the Young's module.

$$\varepsilon_1 = -\varepsilon_5 = \frac{32.D.\left(M_y + F_x.Z1\right)}{E.\pi.\left(D^4 - d^4\right)} \tag{1}$$

$$\varepsilon_{17} = - \varepsilon_{21} = \frac{32.D.\left(M_y + F_x.Z3\right)}{E.\pi.\left(D^4 - d^4\right)} \quad (2)$$

The relation between the output V_{o1} and the supply V_s voltage for measurement of the force F_x is calculated by (3), where it can be observed that the M_y cross-talk in the output signal is eliminated. The constant K is the gauge factor.

$$\frac{V_{o1}}{V_s} = \frac{16.K.F_x.\left(Z3 - Z1\right)}{E.\pi.\left(D^4 - d^4\right)} \quad (3)$$

2.1.2. Theoretical output of the F_y Wheatstone bridge

The measurement of the force F_y is performed by a full Wheatstone bridge, which is composed for the strain gauges number 4, 8, 19 and 23. These gauges were fixed on levels *Z1* and *Z3* in order to eliminate the influence of the moment M_x in the output of the circuit V_{o2}. The strain ε_4, ε_8, ε_{19} *and* ε_{23} of the gauges 4, 8, 19 and 23, respectively, can be calculated by (4) and (5), where E is the Young's module.

$$\varepsilon_4 = - \varepsilon_8 = \frac{32.D.\left(M_y + F_y.Z1\right)}{E.\pi.\left(D^4 - d^4\right)} \quad (4)$$

$$\varepsilon_{19} = - \varepsilon_{23} = \frac{32.D.\left(M_y + F_y.Z3\right)}{E.\pi.\left(D^4 - d^4\right)} \quad (5)$$

The relation between the output V_{o2} and the supply V_s voltage for measurement of the force F_y is calculated by (6), where can be observed that the M_x cross-talk in the output signal is eliminated. The constant *K* is the gauge factor.

$$\frac{V_{o2}}{V_s} = \frac{16.K.F_y.\left(Z3 - Z1\right)}{E.\pi.\left(D^4 - d^4\right)} \quad (6)$$

2.1.3. Theoretical output of the F_z Wheatstone bridge

The measurement of the force F_z is performed by a full Wheatstone bridge, which is composed by the strain gauges number 18, 20, 22, 24, 25, 26, 27 and 28. These gauges were fixed on level *Z3*. The strain ε_{18}, ε_{20}, ε_{22}, ε_{24}, ε_{25}, ε_{26}, ε_{27} *and* ε_{28} of the gauges 18, 20, 22, 24, 25, 26, 27 and 28, respectively, can be calculated by (7) and (8), where E is the Young's module and ν is the Poison module.

$$\varepsilon_{18} = \varepsilon_{20} = \varepsilon_{22} = \varepsilon_{24} = \frac{4.F_z}{E.\pi.\left(D^2 - d^2\right)} \quad (7)$$

$$\varepsilon_{25} = \varepsilon_{26} = \varepsilon_{27} = \varepsilon_{28} = \frac{- 4.F_z.\nu}{E.\pi.\left(D^2 - d^2\right)} \quad (8)$$

The relation between the output V_{o3} and the supply V_s voltage for measurement of the force F_z is calculated by (9), where *K* is the gauge factor.

$$\frac{V_{o3}}{V_s} = \frac{4.K.F_{zy}.\left(1 + \nu\right)}{E.\pi.\left(D^2 - d^2\right)} \quad (9)$$

2.1.4. Theoretical output of the M_x Wheatstone bridge

The measurement of the moment M_x is performed by a full Wheatstone bridge, which is composed by the strain gauges number 11, 12, 15 and 16. These gauges were fixed on the intermediate level *Z2*. The strain ε_{11}, ε_{12}, ε_{15} *and* ε_{16} of the gauges 11, 12, 15 and 16, respectively, can be calculated by (10) and (11), where E is the Young's module.

$$\varepsilon_{11} = \varepsilon_{12} = \frac{32.D.\left(M_x - F_y.Z2\right)}{E.\pi.\left(D^4 - d^4\right)} \tag{10}$$

$$\varepsilon_{15} = \varepsilon_{16} = -\frac{32.D.\left(M_x - F_y.Z2\right)}{E.\pi.\left(D^4 - d^4\right)} \tag{11}$$

The relation between the output V_{o4} and the supply V_s voltage for measurement of the moment M_x is calculated by (12), where it can be observed that the F_y cross-talk in the output signal was not eliminated. The constant *K* is the gauge factor.

$$\frac{V_{o4}}{V_s} = \frac{32.K.D.\left(M_x - F_y.Z2\right)}{E.\pi.\left(D^4 - d^4\right)} \tag{12}$$

2.1.5. Theoretical output of the M_y Wheatstone bridge

The measurement of the moment M_y is performed by a full Wheatstone bridge, which is composed by the strain gauges numbers 9, 10, 13 and 14. These gauges were fixed on the intermediate level *Z2*. The strain ε_9, ε_{10}, ε_{13} *and* ε_{14} of the gauges 9, 10, 13 and 14, respectively, can be calculated by (13) and (14), where E is the Young's module.

$$\varepsilon_9 = \varepsilon_{10} = \frac{32.D.\left(M_y - F_x.Z2\right)}{E.\pi.\left(D^4 - d^4\right)} \tag{13}$$

$$\varepsilon_{13} = \varepsilon_{14} = -\frac{32.D.\left(M_y - F_x.Z2\right)}{E.\pi.\left(D^4 - d^4\right)} \tag{14}$$

The relation between the output V_{o5} and the supply V_s voltage for measurement of the moment M_y is calculated by (15), where it can be observed that the F_x cross-talk in the output signal was not eliminated. The constant *K* is the gauge factor.

$$\frac{V_{o5}}{V_s} = \frac{32.K.D.\left(M_y - F_x.Z2\right)}{E.\pi.\left(D^4 - d^4\right)} \tag{15}$$

2.1.6. Theoretical output of the M_z Wheatstone bridge

The measurement of the moment M_z is performed by a full Wheatstone bridge, which is composed by the strain gauges numbers 2, 3, 6 and 7. These gauges were fixed on level Z1. The strain ε_2, ε_3, ε_6 *and* ε_7 of the gauges 2, 3, 6 and 7, respectively, can be calculated by (16) and (17), where G is the shear module.

$$\varepsilon_2 = \varepsilon_6 = -\frac{8.D.M_z}{G.\pi.\left(D^4 - d^4\right)} \tag{16}$$

$$\varepsilon_3 = \varepsilon_7 = \frac{8.D.M_z}{G.\pi.\left(D^4 - d^4\right)} \tag{17}$$

The relation between the output V_{o6} and the supply V_s voltage for measurement of the moment M_z is calculated by (18), where *K* is the gauge factor.

$$\frac{V_{o6}}{V_s} = \frac{8.K.D.M_z}{G.\pi.\left(D^4 - d^4\right)} \tag{18}$$

2.2. Transducer material and design

The photo of the transducer prototype proposed in this work is presented in Fig. 3. This transducer was built from an aluminium cylinder with Young's module of 73 GPa and Poisson's coefficient equal to 0.33. These properties correspond to the 2024 aluminum alloy, the material from where the prosthesis are made.

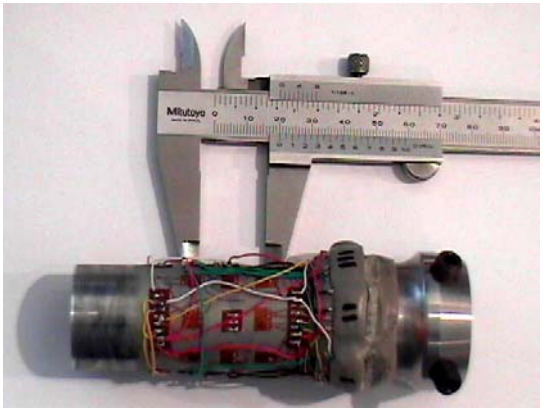

Figure 3. Three-axial transducer prototype.

2.3. Calibration

The three-axial transducer has six output signals (SF_x, SF_y, SF_z, SM_x, SM_y, SM_z) related to the loads applied (F_x, F_y, F_z, M_x, M_y, M_z). If *S* is the vector of the output signal and *F* is the vector of calibration loads, there is a matrix *C* that transforms *S* in *F* (19). It is the calibration matrix of the transducer.

$$F = C.S \tag{19}$$

This matrix *C* has a 6x6 dimension and is determined by (20), where: the elements in the main diagonal are related to the influence of the loads on their respective channel, and the other elements are related to the cross-talk effect. The calibration matrix *C* is determined by (20).

$$\begin{aligned} &F = C.S \\ &F.S^T = C.S.S^T \\ &F.S^T.(S.S^T)^{-1} = C.S.S^T.(S.S^T)^{-1} \\ &C = F.S^T.(S.S^T)^{-1} \end{aligned} \tag{20}$$

The calibration curves of each output channel are presented in Fig. 4 and the other results like hysteresis and repeatability are presented in Tab. 2.

Table 2. Calibration results.

Output	Sensibility [N/mV]	Non-Linearity (1) [% ML]	Hysteresis (1) [% ML]	Repeatability (1) [% ML]
V_{o1}	2.08	1.30	0.68	2.54
V_{o2}	2.20	1.99	2.26	3.33
V_{o3}	5.13	0.24	0.77	1.15
V_{o4}	0.03	0.34	1.90	2.31
V_{o5}	0.03	0.23	0.23	1.87
V_{o6}	0.04	0.33	1.04	2.28

(1) [% ML] = Percent of maximum calibration load.

Copyright © 2005 by ABCM

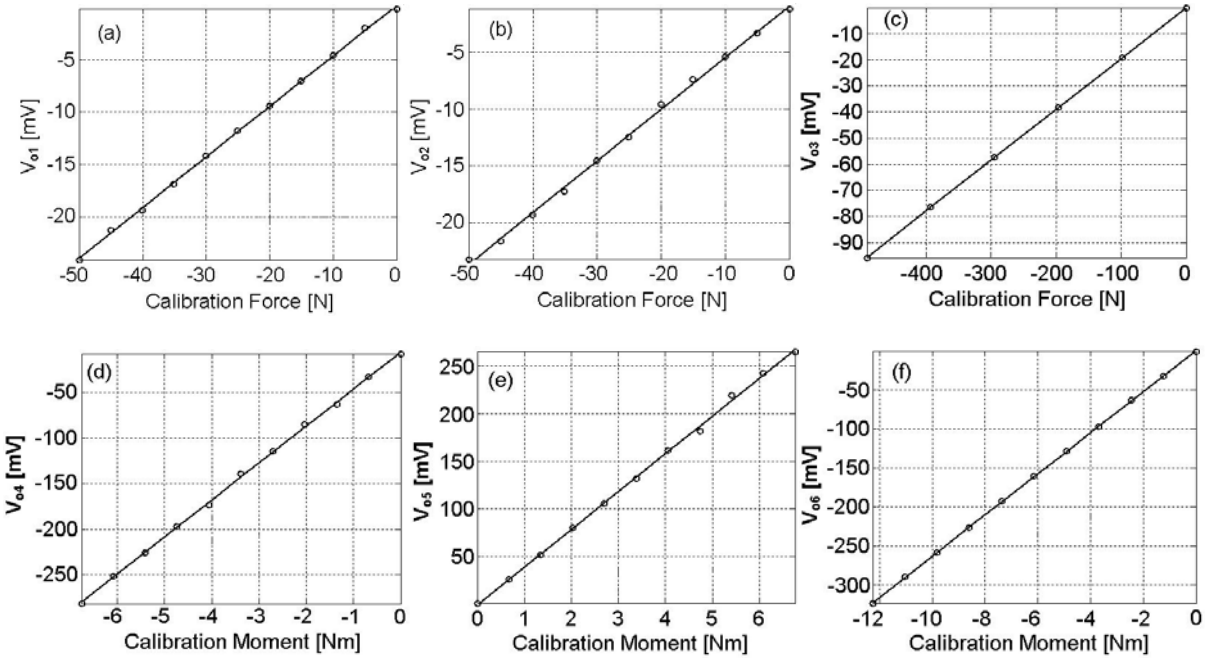

Figure 4. Calibration curves.

2.4. Control group

The amputee subject selection was based upon the following criteria: unilateral trans-femoral amputation without serious complications, one year experience with a definitive prosthesis, and be able to walk at a comfortable speed without auxiliary devices. One man with the above knee amputation was analyzed in this work. This volunteer is 38 years old and has 64 kg. His space-time parameters are: 1.19 s of cycle, 0.79 s of support, 1.18 of stride length, 0.59 of step length, 0.11 of base width and 101.45 steps/min of cadence. The amputee uses one degree of freedom knee (single axis) and a Sach foot.

2.5. Experimental protocol

During the amputee tests the tub between the prosthetic foot and knee was changed to a short tub and the load cell as shown in Fig. 5. The signal-conditioning box was fixed in the waist of the volunteer through an adjustable belt. The signals were sent for the analogical-digital converter through an electrical cable. A specific software built in Delphi 5® was applied in this analysis. These tests were built in a safety place and with the permission of the volunteer.

Figure 5. Three-axial transducer in the amputee.

3. Results and discussion

The force measurement in the posterior-anterior axis (perpendicular of sagittal plane) during some cycles is presented in Fig. 6 (left). Through these curves the anterior force during the initial contact and load response phases can be observed, as the posterior force during pre-swing. The measurement moment around the lateral-medial axis (in the sagittal plane) during some cycles is presented in Fig. 6 (right), where a delay of the extension moment can be observed.

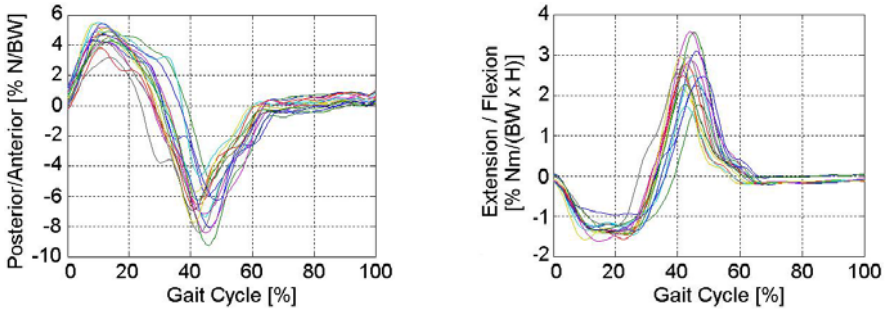

Figure 6. Amputee anterior-posterior force (left) and Amputee sagittal moment (right).

The force measurement in the medial-lateral axis (perpendicular of frontal plane) during some cycles is presented in Fig. 7 (left). Through these curves a support phase of approximately 50% of the gait cycle can be observed. The measurement moment around the anterior-posterior axis (in the frontal plane) during some cycles is presented in Fig. 7 (right), where the predominance of eversion moment during the cycles can be observed.

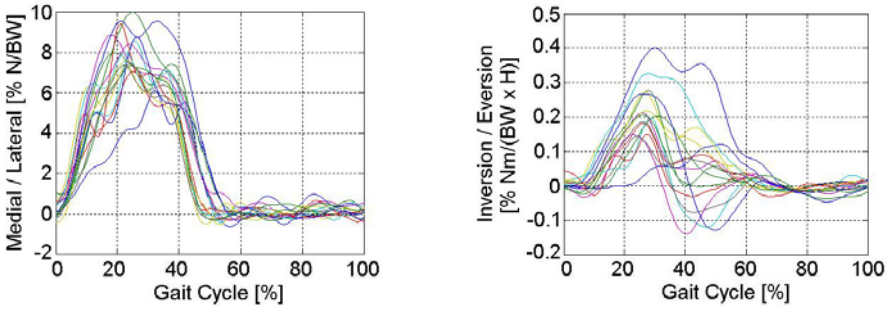

Figure 7. Amputee medial-lateral force (left) and amputee frontal moment (right).

The force measurement in the longitudinal axis (in the tub direction) during some cycles is presented in Fig. 8 (left). Through these curves the gradual transfer of weight from de natural to the amputee leg can be observed. The measurement moment around the longitudinal axis (in the transverse plane) during some cycles is presented in Fig. 8 (right).

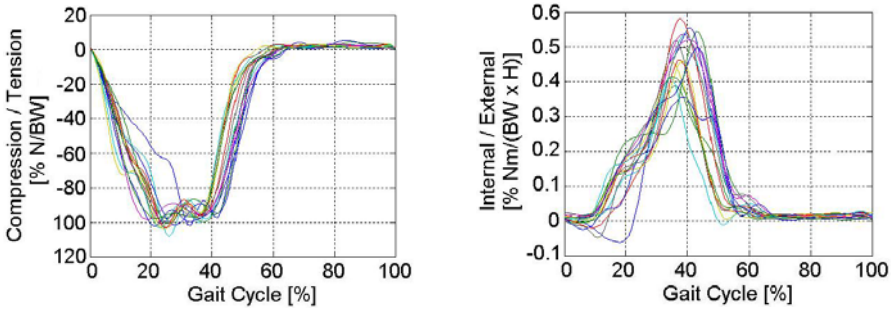

Figure 8. Amputee longitudinal force (left) and amputee transverse moment (right).

4. Conclusion

This work presents a design, construction, calibration and application of a three-axial transducer of forces and moments. It was composed by six full Wheatstone bridges with 28 strain gauges fixed on the external surface of an aluminium alloy cylinder, the same structure used in the prosthetics devices. This transducer was calibrated and presented good results for linearity, hysteresis and repeatability. The tests with an above-knee amputee confirmed the applicability of the proposed system to analyze amputee gait.

5. Acknowledgements

The authors would like to express their gratitude to CAPES for the financial support provided during the course of this research.

Copyright © 2005 by ABCM

6. References

Berme, N., Lawes, P., Solomonidis, S., Paul, J.P., 1976. A short pylon transducer for measurement of prosthetic forces and moments during amputee gait. Engineering in Medicine, v. 4, n. 4, pp. 6 – 8.

Chao, L.P., Yin, C.Y, 1999. The six-component force sensor for measuring the loading of the feet in locomotion, Materials and Design (20), pp. 237 – 244.

Cunningham, D.M, Brown, G.W., 1952. Two devices for measuring the forces acting on the human body during walking, Proc. SESA, 14 (2), pp. 75 – 90.

Hatamura, Y., Matsumoto, K., Morishita, H., 1989. A miniature 6-axis force sensor of multi-layer parallel plate structure, in: Proc. Comf. IMEKO, pp. 567 – 582.

Kim, G.S., Kang, D.I, Jeoung, S.Y., Joo, J.W., 1997. Design of sensing element for 3-component load cell using parallel plate structure, KSME 21 (11), pp. 1871 – 1884.

Kim, G.S., Kang, D.I., Rhee, S.H, 1999. Design and fabrication of a six-component force/moment sensor, Sensors and Actuators (77), pp. 209 – 220.

Kim, J.H., Kang, D.I., Shin, H.H., Park, Y.K., 2003. Design and analysis of a column type multi-component force/moment sensor, Measurement (33), pp. 213 – 219.

Lower, P.J., 1969. Knee Mechanism Performance in Amputee Activity, Ph.D. Thesis, University of Strathclyde.

Ono, K., Hatamura, Y., 1986. A new design for 6-component force/torque sensors, Mechanical Problems in Measurement Force and Mass, pp. 39 – 48.

Scwarzinger, C., Supper, L., Winsauer, H., 1992. Strain gages as sensors for controlling the manipulative robot hand OEDIPUS, Rep. Appl. Measure (8), p. 17 – 28.

Ybuki, A., 1990. Six-axis force/torque sensor for assembly robots, FUJTSU Sci. Technol. J. 26 (1), pp. 41 – 47.

7. Responsibility notice

The authors are the only responsible for the printed material included in this paper.